ACS OMEGA

Article

http://pubs.acs.org/journal/acsodf

Rocking Chair Desalination Battery Based on Prussian Blue Electrodes

Jaehan Lee,[†] Seonghwan Kim,[†] and Jeyong Yoon*[,†,‡]

[†]School of Chemical and Biological Engineering, College of Engineering, Institute of Chemical Process and [‡]Asian Institute for Energy, Environment & Sustainability (AIEES), Seoul National University (SNU), 1 Gwanak-ro, Gwanak-gu, Seoul 151-742, Republic of Korea

Supporting Information

ABSTRACT: The demand for fresh water has been increasing, caused by the growing population and industrialization throughout the world. In this study, we report a capacitive-based desalination system using Prussian blue materials in a rocking chair desalination battery, which is composed of sodium nickel hexacyanoferrate (NaNiHCF) and sodium iron HCF (NaFeHCF) electrodes. In this system, ions are removed not only by charging steps but also by discharging steps, and it is possible to treat actual seawater with this system because the Prussian blue material has a high charge capacity with a reversible reaction of alkaline cations. Here, we demonstrate a rocking chair desalination battery to desalt seawater, and the results show that this system has a high desalination capacity (59.9 mg/g) with efficient energy consumption (0.34 Wh/L for 40% Na ion removal efficiency).

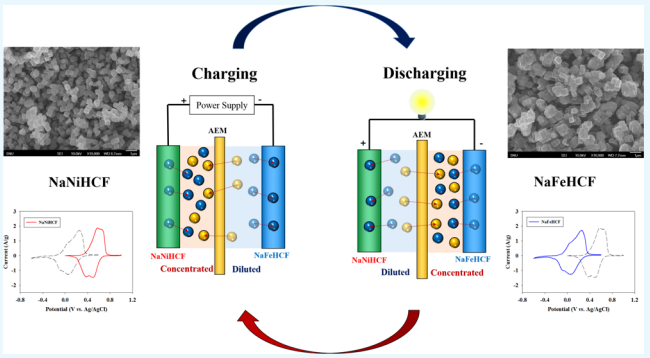

1. INTRODUCTION

The demand for fresh water has been increasing, caused by the growing population and industrialization throughout the world, which has led to the importance of securing water resources. However, the amount of available fresh water has been decreasing due to environmental contamination and climate change. Currently, converting seawater to fresh water is considered to be a solution for the water shortage crisis because the oceans comprise over 97% of the water on the earth. Therefore, the development of a desalination technology is required for a sustainable water supply.[1−3] Seawater desalination technologies using thermal distillation and reverse osmosis (RO) have been investigated but require high power (3−4 kW for 0.7 m^3/h fresh water production),[4] high operation costs for membrane replacement, and large-scale infrastructure, which limit their application in underdeveloped countries and small islands. In addition, the energy consumption of conventional desalination processes is still high, even though RO is presently considered to be the most energy-efficient desalination technology for desalting seawater (3−4 Wh/L).[3−8] Therefore, the development of a novel desalination technology that is energy efficient and convenient to operate with simple equipment is necessary.

To overcome the limitations of a conventional desalination process, capacitive-based electrochemical desalination techniques have been of interest as alternative desalination processes because of their high energy efficiency for brackish water deionization (∼1 g TDS/L),[6] simple equipment, and environmentally friendly characteristics. Capacitive deionization (CDI) is one of many electrochemical desalination technologies that use carbon materials, and ions from salt water are removed by electrical adsorption on the surface of electrodes.[2,6,9−23] Although CDI shows good performance to desalt brackish water, it is difficult to apply for the desalination of high-salt-concentration solutions because the amount of salt adsorption is limited by the capacity of the carbon materials.

Recently, battery material-based desalination techniques, such as a desalination battery,[24] hybrid capacitive deionization (HCDI),[25,26] and symmetric Na-ion desalination (NID) systems,[27] have been reported for treating high-salinity water; in these systems, ions are removed by a chemical reaction with the battery materials. A desalination battery, which is the first seawater desalination system to use battery materials, consists of sodium manganese oxide ($Na_2Mn_5O_{10}$) and silver electrodes. In this system, sodium and chloride ions are captured by the chemical reaction, and it is operated by a four-step charge/discharge process. During the charging process (step 1), the ions in seawater are removed by the intercalation reaction of sodium manganese oxide and the silver/silver chloride reaction. After exchange of the deionized water with the source water (step 2), the discharged cells are recharged, releasing captured ions and producing a concentrated solution (step 3). The brine is then exchanged with the source water, and the cell is ready for the desalination step (step 4). Although the battery system

Received: December 19, 2016
Accepted: April 13, 2017
Published: April 26, 2017

DOI: 10.1021/acsomega.6b00526
ACS Omega 2017, 2, 1653−1659

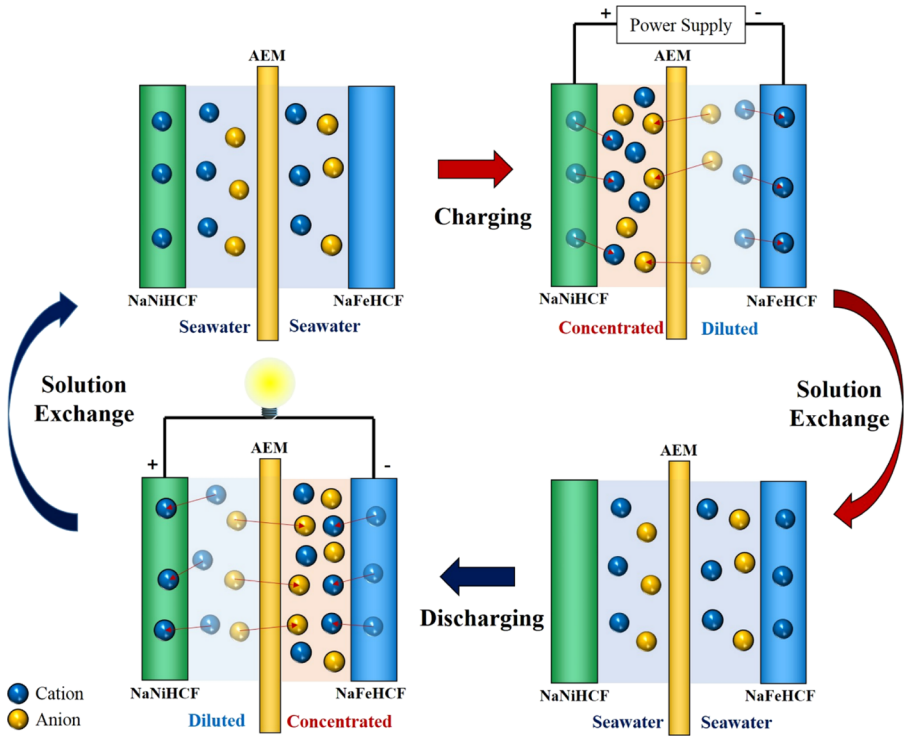

Figure 1. Principle of a rocking chair desalination battery. In the charging step, the cations in the negative compartment solution are captured by a chemical reaction with the negative electrode, whereas cations intercalated into the positive electrode are released into the positive compartment solution. Anions in the negative compartment solution pass through the anion-exchange membrane by diffusion. After exchange of the treated water with the source water, the solutions are diluted and concentrated by the reverse movement of ions during the discharging step.

has an efficient energy consumption for seawater desalination (0.29 Wh/L for the 25% salt-removal efficiency),[24] its economic impact is limited due to the high price of silver. The HCDI system uses a battery electrode, an anion-exchange membrane, and an activated carbon electrode. The ion removal performance of the HCDI system shows a high ion removal capacity and a rapid ion removal rate compared to those of a typical CDI, but the ion removal capacity of HCDI is still limited by the carbon material. Symmetric NID is a simulated system that operates in a similar manner to electrodialysis using a porous sodium manganese oxide ($Na_{0.44}MnO_2$) electrode with an anion-selective membrane. In this system, Na ions are captured in the battery material, whereas Cl ions are removed by diffusion through the anion-selective membrane. From the modeling data, NID has a remarkable energy efficiency (0.74 kWh/m^3 for seawater-level NaCl) with the possibility of a high water recovery rate (maximum: 95% water recovery).[27] However, the symmetric system is difficult to use due to the uncertain charging/discharging step but also because $Na_{0.44}MnO_2$ has a low specific charge capacity (35 mAh/g); there are also competing intercalation reactions with alkaline cations (K^+, Mg^{2+}, and Ca^{2+}).

Here, we investigated a novel, simple, and high-efficiency desalination system using Prussian blue electrodes. Figure 1 represents the principle of the rocking chair desalination battery; this system consists of sodium nickel hexacyanoferrate (NaNiHCF) and sodium iron HCF (NaFeHCF) electrodes for capturing cations, and there are two solution compartments, which are formed by an anion-exchange membrane in the cell. The system operates similar to rocking chair batteries, as shown by the movement of ions during the charging and discharging steps; however, the anion-exchange membrane blocks cation movement into another solution, whereas anions pass through the anion-exchange membrane by diffusion, inducing a charge imbalance of the solutions. From the ion movement in the cell, the solutions are concentrated and diluted during both the charging and discharging steps, and it does not require a regeneration step that creates brine in a desalination battery. Prussian blue analogues $A_xM[Fe(CN)_6]$ (A: alkali cations, M: transition metal ions) have an open framework structure with the large cages surrounded by an Fe—C≡N—Fe bridge, and it allows to react with various cations, including K^+, Mg^{2+}, and Ca^{2+}, which are the main alkaline ions in seawater.[28,29] They are suitable materials for aqueous batteries because of their reversible reaction, long life cycle, and high specific capacity.[30,31] Furthermore, they have the characteristics of being environmentally benign and of low cost,[32] meaning that they can be applied for the capacitive-based desalination technology. In this work, a rocking chair desalination battery that consists of two Prussian blue materials was used for the electrochemical desalination process, and the salt removal performance and electrochemical properties were evaluated using actual seawater.

2. EXPERIMENTAL SECTION

2.1. Synthesis of Prussian Blue Materials. The Prussian blue materials used in this study were synthesized by a controlled crystallization reaction with citrate ions to obtain an ordered nanocube structure. NaNiHCF particles were prepared by mixing 100 mL of a 0.05 M $NiCl_2$ + 0.35 M Na-citrate solution and 100 mL of a 0.05 M $Na_4Fe(CN)_6$ solution under vigorous stirring. The reaction was carried out for 24 h at room temperature, and the obtained solution was aged for 20 h at room temperature. The precipitated products were filtered and

DOI: 10.1021/acsomega.6b00526
ACS Omega 2017, 2, 1653−1659

washed with distilled water and ethanol several times, and the collected particles were dried in an oven at 70 °C under a vacuum condition. NaFeHCF particles were synthesized by mixing 100 mL of a 0.05 M $FeCl_2$ + 0.20 M Na-citrate solution and 100 mL of a 0.05 M $Na_4Fe(CN)_6$ solution. The mixing solution was stirred for 3 h and aged for 20 h at room temperature. The resulting particles were filtered and rinsed with distilled water and ethanol several times and then dried in an oven at 70 °C to eliminate the remaining solvent. The prepared particles were characterized using inductively coupled plasma atomic emission spectrometer (ICP-AES; VARIAN 730ES, Australia), field emission scanning electron microscopy (FESEM; JEOL JSM 6700 F, Japan), and X-ray powder diffraction (D8 Discover). All of the reagents were purchased from Sigma-Aldrich Corporation.

2.2. Electrode Fabrication and Cell Assembly. The NaNiHCF and NaFeHCF electrodes were made by mixing 70 wt % active material, 20 wt % carbon black (Super P, Timcal, Switzerland), and 10 wt % poly(tetrafluoroethylene) (PTFE; Sigma-Aldrich) in an ethanol solvent. The resulting slurry was pressed using a roll press machine to obtain sheet-type electrodes with a thickness of approximately 300 μm. The fabricated Prussian blue electrodes were dried using a vacuum oven at 60 °C for 12 h to eliminate the remaining solvent. Rectangular-shaped NaNiHCF (2.0 cm × 2.0 cm, weight: 90 ± 5 mg) was used as the positive electrode, and the same-sized NaFeHCF (2.0 cm × 2.0 cm, weight: 86 ± 4 mg) rectangle was used as a negative electrode. The Prussian blue electrodes were attached onto titanium plates (thickness: 0.20 mm; Sigma-Aldrich) using carbon paint (DAG-T-502; Ted Pella). The rocking chair desalination battery consisted of two Prussian blue electrodes, an anion-exchange membrane (AMX; ASTOM Co., Japan), and polyamide woven spacers (2.0 cm × 2.0 cm, thickness: 0.6 mm). The electrolyte of the cell consisted of a positive-electrode compartment and a negative-electrode compartment divided by the anion-exchange membrane, as shown in Figure S3, and the volume of each compartment is approximately 0.4 cm^3. Before assembling the cell, the NaFeHCF electrode was charged to 0.3 V for 30 min in a 0.5 M NaCl solution using a three-electrode cell with a Ag/AgCl (KCl sat′) reference electrode and a stainless steel counter electrode to extract Na ions from NaFeHCF to obtain a ready-to-use negative electrode. The cell was covered by a PTFE plate and silicon rubber. To avoid the negative cell voltage during the discharging step, the battery cell was precharged in a 0.5 M NaCl solution at a constant current (2 mA) for 10 min before starting the test. The seawater used in this study was obtained from the East Sea (Sockcho, Gangwon Province, Korea).

2.3. Desalination Performance Test. To probe the possibility of application for seawater desalination processes, 0.6 mL of seawater was put into the positive and negative compartment of the cell (0.3 mL in each compartment). The desalination process was conducted at a constant current (±0.5 mA/cm^2) for 1 h (removal of 40% Na ions) and 40 min (removal of 25% Na ions). Each solution in the positive and negative compartments was extracted and exchanged with virgin seawater (0.3 mL in each compartment) by reassembling the cell after the charging and discharging processes. To investigate the maximum ion removal capacity, an additional experiment was carried out at constant current operation (±0.5 mA/cm^2) in a 0.5 M NaCl aqueous solution with a voltage range of 0.05−0.85 V, and the results of the desalination performance are provided in the Supporting Information (see Figure S2 and Table S2). The concentration of various ions was measured by ion chromatography (ICS-1100 and DX-120; Dionex) with 50 μL of samples after each process. The desalination results from triplicate experiments with standard deviations are presented in this work.

Energy consumption during the operation can be calculated by the amount of energy consumed during the charging step minus the energy generated during the discharging step and is demonstrated by the path integral of a voltage versus charge plot, as given by previous research[24,33−36]

$$W = \oint_c \Delta V \, dq \tag{1}$$

where ΔV is the cell voltage (V) and q is the charge (C) during the operation.

The ion removal efficiency reported in the table is based on the equation

$$\text{ion removal } (\%) = \frac{c_i - c_t}{c_i} \times 100 \tag{2}$$

where c_i is the ion concentration of the initial source water and c_t is the ion concentration of treated water. The Na ion removal efficiency of the solution was represented by the average removal efficiency percent of Na ions by repeating the first cycle of the system using virgin Prussian blue electrodes.

The efficiency of salt removal per total charge is expressed by the Coulombic efficiency according to the following equation

$$\eta_c \ (\%) = \frac{z_i F(n_I - n_F)}{\sum} \times 100 \tag{3}$$

where z_i is the ion valance, F is the Faraday constant, $n_I - n_F$ is the molar change in ions, and $\sum$ is the total charge transferred at the charging and discharging steps.

2.4. Electrochemical Characterization. The electrochemical performance of the Prussian blue electrodes was examined in an electrochemical cell that was manufactured with a pair of graphite current collectors (d = 18 mm) and a glass fiber separator (GF/A; Whatman), as shown in the Supporting Information (see Figure S4). Cyclic voltammetry (CV) was performed in a 1 M NaCl solution or seawater with a three-electrode system. Round Prussian blue electrodes (d = 9 mm) were used as the working electrode, and the reference electrode was a Ag/AgCl (KCl sat′) electrode. A sheet-type Ag/AgCl electrode (d = 18 mm) with a large specific capacity was used as the counter electrode. Galvanostatic charging/discharging tests were carried out using a two-electrode or three-electrode cell in seawater electrolytes, and, before the test, 0.3 V (vs Ag/AgCl) was applied to the NaFeHCF electrode for 30 min in a 0.5 M NaCl solution. NaNiHCF and NaFeHCF electrodes were used as positive and negative electrodes. In a three-electrode cell, a Ag/AgCl (KCl sat′) electrode was used. To examine the stability of the NaNiHCF and NaFeHCF cell in seawater, a galvanostatic cycling test was conducted in an electrochemical cell at a current of ±1.05 mA (0.1 A/g of NaFeHCF) in a voltage range of 0.10−0.80 V. The electrochemical analyses were conducted using a battery cycler (WBCS3000; WonA Tech, Korea).

3. RESULTS AND DISCUSSION

Figure 2a,b shows the voltage profiles during the charging and discharging steps at a current density of ±0.5 mA/cm^2 for 1 h

DOI: 10.1021/acsomega.6b00526
ACS Omega 2017, 2, 1653−1659

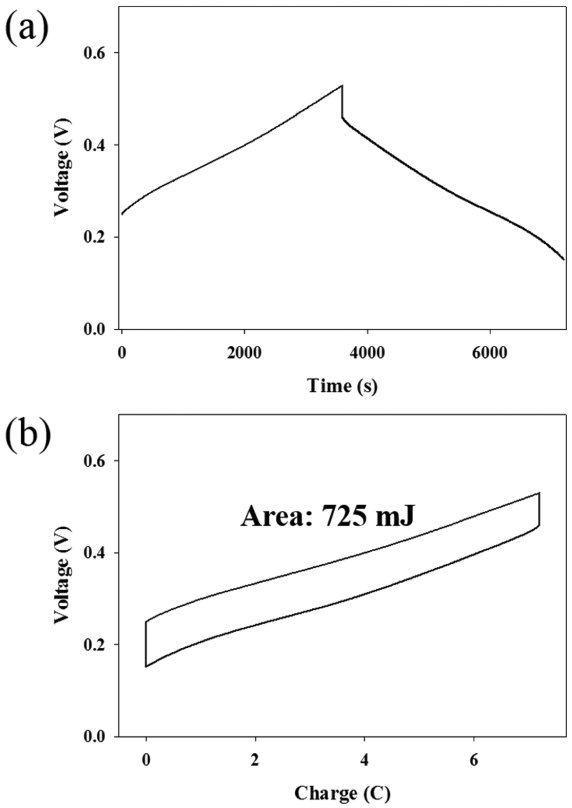

Figure 2. (a) Voltage profile with time during the charging/discharging steps of a rocking chair desalination battery and (b) a voltage vs charge plot during the desalination cycle in seawater (current density: 0.5 mA/cm^2).

in seawater, as well as the corresponding voltage versus charge plots, respectively. As shown in Figure 2a, the NaNiHCF/NaFeHCF cell shows a reversible redox reaction in the seawater electrolyte, and it is indicated that the cell can work as a secondary battery during the desalination process. The electrochemical reaction during the charging and discharging process is as follows

charging

$$\text{positive electrode: } Na_{x_1}Ni[Fe(CN)_6] \rightarrow Na_{x_1-x}Ni[Fe(CN)_6] + xNa^+ \quad (4)$$

$$\text{negative electrode: } Na_{x_2}Fe[Fe(CN)_6] + x_{sol(-)}Na^+ \rightarrow Na_{x_2+x_{sol(-)}}Fe[Fe(CN)_6] \quad (5)$$

discharging

$$\text{positive electrode: } Na_{x_3}Ni[Fe(CN)_6] + x_{sol(+)}Na^+ \rightarrow Na_{x_3+x_{sol(+)}}Ni[Fe(CN)_6] \quad (6)$$

$$\text{negative electrode: } Na_{x_4}Fe[Fe(CN)_6] \rightarrow Na_{x_4-y}Fe[Fe(CN)_6] + yNa^+ \quad (7)$$

where $x_{sol(-)}Na^+$ is the sodium ions in the negative compartment and intercalated into the NaFeHCF electrode, and $x_{sol(+)}Na^+$ is the sodium ions in positive compartment and intercalated into the NaNiHCF electrode. From the property of the Prussian blue electrode, it can be observed that cations in the solution are intercalated into the electrode, whereas cations inserted at another electrode are released into the solution. The NaNiHCF/NaFeHCF cell operates as a rocking chair battery, and it is possible to desalt a solution not only during charging but also during discharging, by adding an anion-selective membrane. If a conventional porous separator is used instead of anion-exchange membrane, a desalination performance of the system would be limited by cation movement into another compartment during the operation. The voltage drop (approximately 0.06 V) between the charging and discharging steps indicates the polarization though the solid−liquid interface and resistance in the cell caused by the electrode, the electrolyte, and the ion-exchange membrane.

Table 1 shows the various ion concentrations of source water (seawater) and a desalted solution during the charging or discharging steps. From the ion concentration changes of the dilute solution, the battery system can desalt the source water not only when discharging but also when charging the system. The average removal efficiency of Na ions during one cycle, which is a major component of seawater, is approximately 40%. The total energy consumed during the operation is 725 mJ (deionized water volume: 0.6 mL), and the energy required per 1 L of seawater is 0.34 Wh with 50% water recovery (the percent of seawater converted to treated water). The Coulombic efficiencies of cations and anions are 83.5 and 83.1%, respectively. The observed desalination performance of the system demonstrates that it can desalt both monovalent and multivalent ions because the Prussian blue materials have different reversible intercalation and deintercalation potentials with various cations.[29] Considering the number of desalting ions, the Prussian blue materials have a higher affinity for monovalent ions than multivalent ions due to the expectation of electrostatic repulsion.[37] To compare the desalination performance to that of a previous study, we carried out an additional experiment in which the average Na removal efficiency was approximately 25% using seawater (see Figure S1 and Table S1). The energy consumed during the desalination process is 299 mJ during one cycle, and the energy required for treating 1 L of seawater is 0.14 Wh. This

Table 1. Various Ion Concentrations and Ion Removal Efficiencies for Seawater and Dilute Solutions

	Na^+	K^+	Mg^{2+}	Ca^{2+}	Cl^-	SO_4^{2-}
seawater (mM)	477.5	10.8	58.9	11.1	512.1	31.5
dilute solution (charging, mM)	291.5 ± 8.6	0.9 ± 0.4	56.7 ± 1.2	9.8 ± 0.3	314.8 ± 13.9	27.8 ± 0.9
dilute solution (discharging, mM)	283.1 ± 15.5	1.3 ± 0.6	56.5 ± 1.8	10.2 ± 0.3	310.1 ± 15.6	28.2 ± 1.2
ion removal (average, mM)	190.2	9.7	2.7	1.2	199.7	3.5
ion removal (average, %)	39.9	90.1	4.5	10.5	39.0	11.0

DOI: 10.1021/acsomega.6b00526
ACS Omega 2017, 2, 1653−1659

value is a remarkable result compared to that of previous research using a battery system (0.29 Wh/L).[24]

The maximum desalination capacity, which is an important parameter in capacitive-based electrochemical desalination technologies (calculated as the mass of deionized NaCl (mg) divided by the total mass of the electrodes (g)), was measured from an additional test at a voltage range of 0.05−0.85 V in a 0.5 M NaCl aqueous solution (see Figure S2 and Table S2). From one cycle of the desalination process, the average deionized NaCl concentration is 298 mM and the desalination capacity is approximately 59.9 mg/g. Note that the mass of salt removal in the system was the total amount of deionized NaCl during one cycle of the process (charging and discharging steps). This excellent desalination performance is explained by the fact that the system can deionize the source water during both the charging and discharging steps, as it overcomes a limitation of energy efficiency and capacity among electrochemical desalination processes, which have a separate regeneration and create brine.

Figure 3a,b shows the FESEM images of as-prepared NaNiHCF and NaFeHCF. To obtain ordered nanocube particles, we synthesized Prussian blue materials using kinetically controlled crystallization, which is a controllable crystal growth method that uses the addition of sodium citrate, as reported in previous research.[38,39] In this method, sodium citrate served as a chelating agent that is coordinated with metal ions, and, then, the slowly released metal ions from the citrate complex are reacted with hexacyanoferrate ions. This slow nucleation and crystal growth allows for the formation of well-shaped nanocube particles, and the particle size can be controlled by adjusting the amount of citrate ions. From the SEM images, the morphology of the Prussian blue particles appears to be a well-crystallized nanocube structure that has a size distribution of 300−500 nm. Figure 3c shows the XRD patterns of the as-prepared NaNiHCF and NaFeHCF. The XRD pattern of NaNiHCF reveals that diffraction lines of NaNiHCF with indexes of 220, 420, 440, and 620 exhibit as a doublet by comparison with the structured $Fe_4[Fe(CN)_6]_3$ (JCPDS 52-1970). Supported by the ICP-AES analysis results (the Na/(Ni + Fe) molar ratio of NaNiHCF and the Na/Fe molar ratio of NaFeHCF are 0.85/1 and 0.72/1, respectively), this distortion of the face-centered cubic (fcc) structure is interpreted by the presence of an excess amount of Na ions in the Prussian blue lattice, which indicates a rhombohedral structure.[40−42] The XRD peaks of NaFeHCF have a strong line and are well indexed to an fcc structure (JCDPDS 73-0687), which indicates the high crystallinity of NaFeHCF particles.

Figure 4 shows the electrochemical properties of the Prussian blue electrodes characterized by CV and galvanostatic charging/discharging in an electrochemical cell. The CV curves of the NaFeHCF and NaNiHCF electrodes in Figure 4a appear as broad redox peaks between −0.1 to 0.2 V (vs Ag/AgCl) and 0.4 to 0.6 V (vs Ag/AgCl); also, similar redox reaction properties are observed in both 1 M NaCl and seawater electrolytes. As expected from the difference of the redox reaction potential, the rechargeable battery system can be composed of NaNiHCF as a positive electrode and NaFeHCF as a negative electrode. Figure 4b,c shows the galvanostatic performance of the NaNiHCF/NaFeHCF full cell and the potential profiles of each electrode using a three-electrode system with a silver/silver chloride (KCl sat') reference electrode in seawater. Closely related to the CV results, the Prussian blue electrodes exhibit a similar redox reaction

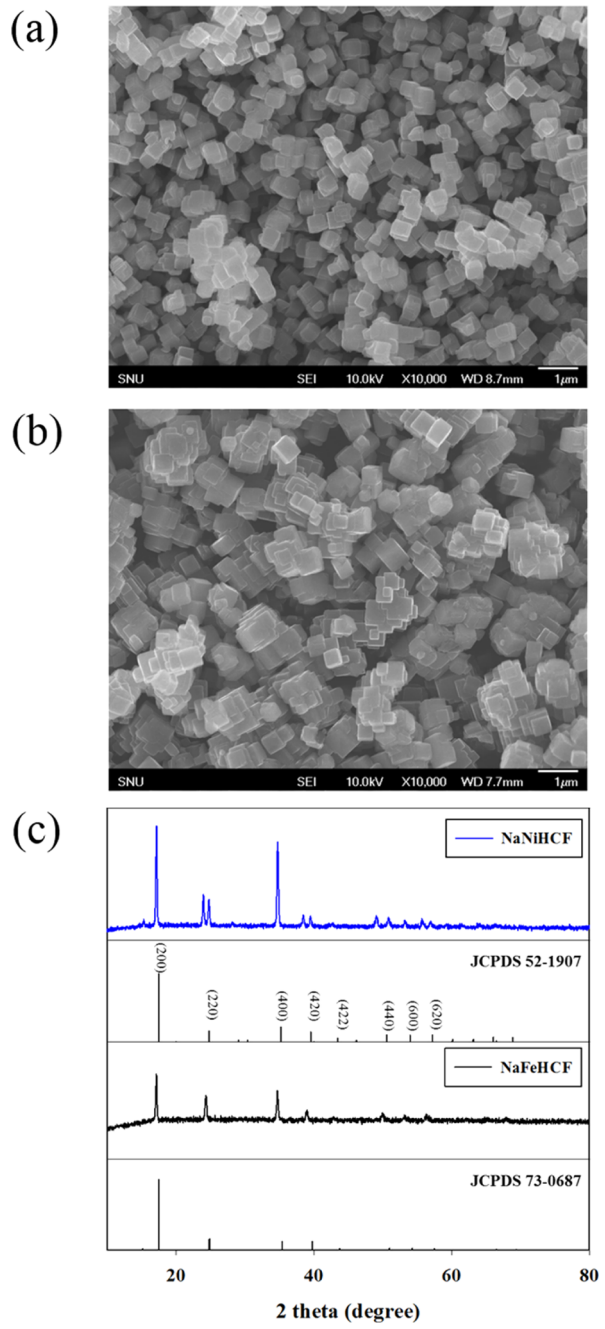

Figure 3. SEM images of (a) NaNiHCF particles and (b) NaFeHCF particles. (c) The XRD patterns of NaNiHCF with reference to JCPDS no. 52-1907 ($Fe_4[Fe(CN)_6]_3$) and NaFeHCF with reference to JCPDS no. 73-0687 ($FeFe(CN)_6$) data.

potential plateau at −0.1 to 0.3 V in the negative electrode and 0.4−0.8 V in the positive electrode.

Figure 4d shows the galvanostatic cycling performance of the NaNiHCF/NaFeHCF full cell at a current density of 0.1 A/$g_{negative}$ between 0.10 and 0.80 V in a seawater solution. As shown in the results, the initial charge capacity was 56.2 mAh/$g_{negative}$, which is higher than that of manganese oxide-based materials, such as $Na_{0.44}MnO_2$ and $Na_2Mn_5O_{10}$ (35 mAh/g), that are used for capacitive-based desalination technologies. The retained capacity remains at 91.5% after 100 cycles, and the Coulombic efficiency stays above 92% (average: 92.9%), indicating its good stability even though the electrolyte was

DOI: 10.1021/acsomega.6b00526
ACS Omega 2017, 2, 1653−1659

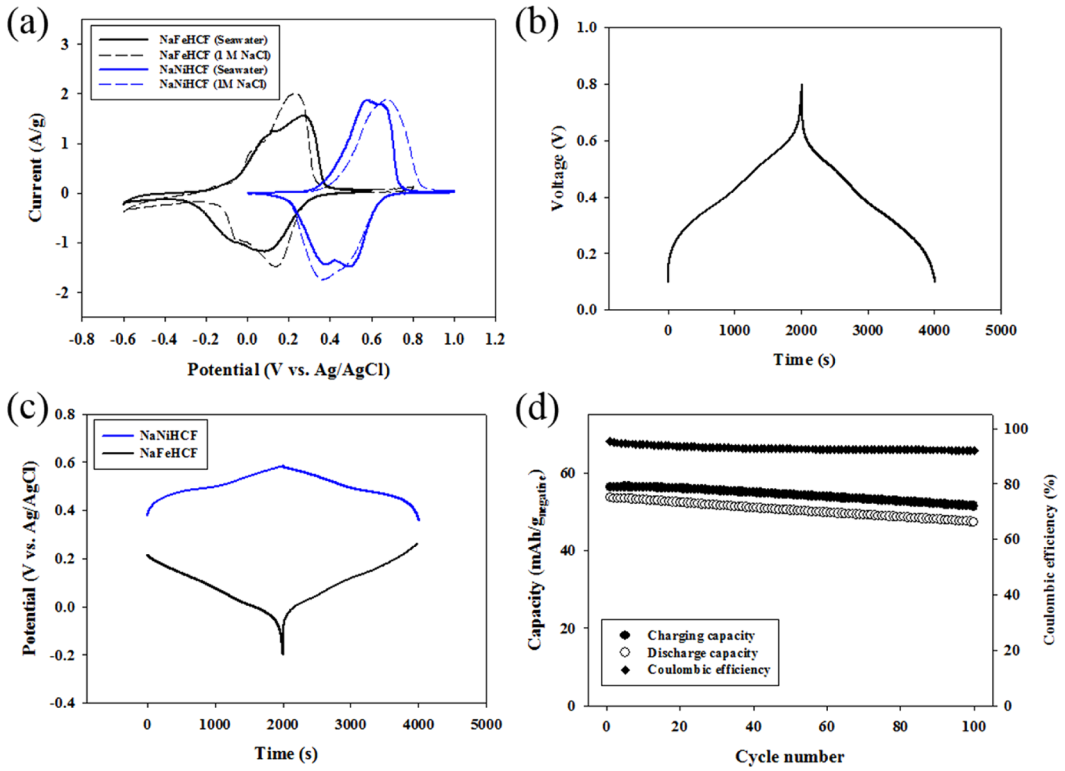

Figure 4. (a) CV curves of NaNiHCF and NaFeHCF electrodes in 1 M of NaCl and a seawater electrolyte (scan rate: 2 mV/s). (b) The voltage profiles of the NaNiHCF/NaFeHCF full cell and (c) potential changes in the three-electrode configuration during the charging/discharging of seawater electrolytes (current density: 0.1 A/$g_{NaFeHCF}$). (d) Galvanostatic cycling performance of the NaNiHCF/NaFeHCF full cell in seawater (current density: 0.1 A/$g_{NaFeHCF}$).

seawater without any oxygen removal treatment. These results suggest that the Prussian blue materials have good cycling stability in a mixed electrolyte solution containing various ion species due to the large size of the open framework structure.[29,30]

4. CONCLUSIONS

In this study, a rocking chair desalination battery was developed using NaNiHCF and NaFeHCF electrodes. This system desalts the source water at both the charge and discharge steps. This principle of the system contributes not only to a high desalination capacity but also efficient energy consumption. As demonstrated in this work, the system shows a high Na ion removal efficiency (40%) and excellent energy efficiency (0.34 Wh/L) for seawater desalination. In addition, it was found that the system has a high desalination capacity (59.9 mg/g) with good stability in seawater. Although the demonstrated work shows low water treatment capacity with a low water recovery ratio, we believe that it is possible to enhance the water treatment capacity with high water recovery after optimization and development of a flow-type reactor.

■ ASSOCIATED CONTENT

Supporting Information

The Supporting Information is available free of charge on the ACS Publications website at DOI: 10.1021/acsomega.6b00526.

Additional experimental results; illustration of a rocking chair desalination battery; the electrochemical cell used in this study (PDF)

■ AUTHOR INFORMATION

Corresponding Author

*E-mail: Jeyong@snu.ac.kr. Phone: +82-2-880-8927. Fax: +82-2-876-8911.

ORCID

Jaehan Lee: 0000-0002-8191-1396

Notes

The authors declare no competing financial interest.

■ ACKNOWLEDGMENTS

This research was supported by a grant (code 16IFIP-B065893-04) from Industrial Facilities & Infrastructure Research Program funded by Ministry of Land, Infrastructure and Transport of Korean government and Basic Science Research Program through the National Research Foundation of Korea (NRF) funded by the Ministry of Education (NRF-2016R1D1A1A02937469).

■ REFERENCES

(1) Shannon, M. A.; Bohn, P. W.; Elimelech, M.; Georgiadis, J. G.; Mariñas, B. J.; Mayes, A. M. Science and technology for water purification in the coming decades. *Nature* **2008**, *452*, 301−310.

(2) Anderson, M. A.; Cudero, A. L.; Palma, J. Capacitive deionization as an electrochemical means of saving energy and delivering clean water. Comparison to present desalination practices: Will it compete? *Electrochim. Acta* **2010**, *55*, 3845−3856.

(3) Kim, S. J.; Ko, S. H.; Kang, K. H.; Han, J. Direct seawater desalination by ion concentration polarization. *Nat. Nanotechnol.* **2010**, *5*, 297−301.

(4) Ntavou, E.; Kosmadakis, G.; Manolakos, D.; Papadakis, G.; Papantonis, D. Experimental evaluation of a multi-skid reverse osmosis

DOI: 10.1021/acsomega.6b00526
ACS Omega 2017, 2, 1653−1659

unit operating at fluctuating power input. *Desalination* **2016**, *398*, 77−86.
(5) Elimelech, M.; Phillip, W. A. The future of seawater desalination: energy, technology, and the environment. *Science* **2011**, *333*, 712−717.
(6) Zhao, R.; Porada, S.; Biesheuvel, P.; Van der Wal, A. Energy consumption in membrane capacitive deionization for different water recoveries and flow rates, and comparison with reverse osmosis. *Desalination* **2013**, *330*, 35−41.
(7) Cho, B.-Y.; Kim, H.-W.; Shin, Y.-S. A Study on boron removal for seawater desalination using the combination process of mineral cluster and RO membrane system. *Environ. Eng. Res.* **2015**, *20*, 285−289.
(8) Kim, H. J.; Lim, M.-Y.; Jung, K. H.; Kim, D.-G.; Lee, J.-C. High-performance reverse osmosis nanocomposite membranes containing the mixture of carbon nanotubes and graphene oxides. *J. Mater. Chem. A* **2015**, *3*, 6798−6809.
(9) Seo, S.-J.; Jeon, H.; Lee, J. K.; Kim, G.-Y.; Park, D.; Nojima, H.; Lee, J.; Moon, S.-H. Investigation on removal of hardness ions by capacitive deionization (CDI) for water softening applications. *Water Res.* **2010**, *44*, 2267−2275.
(10) Suss, M. E.; Baumann, T. F.; Bourcier, W. L.; Spadaccini, C. M.; Rose, K. A.; Santiago, J. G.; Stadermann, M. Capacitive desalination with flow-through electrodes. *Energy Environ. Sci.* **2012**, *5*, 9511−9519.
(11) Jeon, S.-i.; Park, H.-r.; Yeo, J.-g.; Yang, S.; Cho, C. H.; Han, M. H.; Kim, D. K. Desalination via a new membrane capacitive deionization process utilizing flow-electrodes. *Energy Environ. Sci.* **2013**, *6*, 1471−1475.
(12) Kim, Y.-J.; Choi, J.-H. Improvement of desalination efficiency in capacitive deionization using a carbon electrode coated with an ion-exchange polymer. *Water Res.* **2010**, *44*, 990−996.
(13) Porada, S.; Zhao, R.; Van Der Wal, A.; Presser, V.; Biesheuvel, P. Review on the science and technology of water desalination by capacitive deionization. *Prog. Mater. Sci.* **2013**, *58*, 1388−1442.
(14) Kim, C.; Lee, J.; Kim, S.; Yoon, J. TiO2 sol−gel spray method for carbon electrode fabrication to enhance desalination efficiency of capacitive deionization. *Desalination* **2014**, *342*, 70−74.
(15) Suss, M.; Porada, S.; Sun, X.; Biesheuvel, P.; Yoon, J.; Presser, V. Water desalination via capacitive deionization: what is it and what can we expect from it? *Energy Environ. Sci.* **2015**, *8*, 2296−2319.
(16) Xu, X.; Pan, L.; Liu, Y.; Lu, T.; Sun, Z.; Chua, D. H. Facile synthesis of novel graphene sponge for high performance capacitive deionization. *Sci. Rep.* **2015**, *5*, No. 8458.
(17) Zhao, R.; Biesheuvel, P.; Van der Wal, A. Energy consumption and constant current operation in membrane capacitive deionization. *Energy Environ. Sci.* **2012**, *5*, 9520−9527.
(18) Porada, S.; Borchardt, L.; Oschatz, M.; Bryjak, M.; Atchison, J.; Keesman, K.; Kaskel, S.; Biesheuvel, P.; Presser, V. Direct prediction of the desalination performance of porous carbon electrodes for capacitive deionization. *Energy Environ. Sci.* **2013**, *6*, 3700−3712.
(19) Gao, X.; Omosebi, A.; Landon, J.; Liu, K. Surface charge enhanced carbon electrodes for stable and efficient capacitive deionization using inverted adsorption−desorption behavior. *Energy Environ. Sci.* **2015**, *8*, 897−909.
(20) Yeh, C.-L.; Hsi, H.-C.; Li, K.-C.; Hou, C.-H. Improved performance in capacitive deionization of activated carbon electrodes with a tunable mesopore and micropore ratio. *Desalination* **2015**, *367*, 60−68.
(21) Fan, C.-S.; Tseng, S.-C.; Li, K.-C.; Hou, C.-H. Electro-removal of arsenic(III) and arsenic(V) from aqueous solutions by capacitive deionization. *J. Hazard. Mater.* **2016**, *312*, 208−215.
(22) Tsouris, C.; Mayes, R.; Kiggans, J.; Sharma, K.; Yiacoumi, S.; DePaoli, D.; Dai, S. Mesoporous carbon for capacitive deionization of saline water. *Environ. Sci. Technol.* **2011**, *45*, 10243−10249.
(23) Długołęcki, P.; Van Der Wal, A. Energy recovery in membrane capacitive deionization. *Environ. Sci. Technol.* **2013**, *47*, 4904−4910.
(24) Pasta, M.; Wessells, C. D.; Cui, Y.; La Mantia, F. A desalination battery. *Nano Lett.* **2012**, *12*, 839−843.
(25) Lee, J.; Kim, S.; Kim, C.; Yoon, J. Hybrid capacitive deionization to enhance the desalination performance of capacitive techniques. *Energy Environ. Sci.* **2014**, *7*, 3683−3689.
(26) Kim, S.; Lee, J.; Kim, C.; Yoon, J. Na2FeP2O7 as a Novel Material for Hybrid Capacitive Deionization. *Electrochim. Acta* **2016**, *203*, 265−271.
(27) Smith, K. C.; Dmello, R. Na-Ion Desalination (NID) Enabled by Na-Blocking Membranes and Symmetric Na-Intercalation: Porous-Electrode Modeling. *J. Electrochem. Soc.* **2016**, *163*, A530−A539.
(28) Wessells, C. D.; Peddada, S. V.; Huggins, R. A.; Cui, Y. Nickel hexacyanoferrate nanoparticle electrodes for aqueous sodium and potassium ion batteries. *Nano Lett.* **2011**, *11*, 5421−5425.
(29) Wang, R. Y.; Wessells, C. D.; Huggins, R. A.; Cui, Y. Highly reversible open framework nanoscale electrodes for divalent ion batteries. *Nano Lett.* **2013**, *13*, 5748−5752.
(30) Wang, R. Y.; Shyam, B.; Stone, K. H.; Weker, J. N.; Pasta, M.; Lee, H. W.; Toney, M. F.; Cui, Y. Reversible Multivalent (Monovalent, Divalent, Trivalent) Ion Insertion in Open Framework Materials. *Adv. Energy Mater.* **2015**, *5*, No. 1401869.
(31) Liu, Y.; Qiao, Y.; Zhang, W.; Li, Z.; Ji, X.; Miao, L.; Yuan, L.; Hu, X.; Huang, Y. Sodium storage in Na-rich NaxFeFe(CN)$_6$ nanocubes. *Nano Energy* **2015**, *12*, 386−393.
(32) Wu, X.; Cao, Y.; Ai, X.; Qian, J.; Yang, H. A low-cost and environmentally benign aqueous rechargeable sodium-ion battery based on NaTi2(PO4)3−Na2NiFe(CN)6 intercalation chemistry. *Electrochem. Commun.* **2013**, *31*, 145−148.
(33) La Mantia, F.; Pasta, M.; Deshazer, H. D.; Logan, B. E.; Cui, Y. Batteries for efficient energy extraction from a water salinity difference. *Nano Lett.* **2011**, *11*, 1810−1813.
(34) Lee, J.; Yu, S.-H.; Kim, C.; Sung, Y.-E.; Yoon, J. Highly selective lithium recovery from brine using a λ-MnO2−Ag battery. *Phys. Chem. Chem. Phys.* **2013**, *15*, 7690−7695.
(35) Kim, S.; Lee, J.; Kang, J. S.; Jo, K.; Kim, S.; Sung, Y.-E.; Yoon, J. Lithium recovery from brine using a λ-MnO2/activated carbon hybrid supercapacitor system. *Chemosphere* **2015**, *125*, 50−56.
(36) Pasta, M.; Battistel, A.; La Mantia, F. Batteries for lithium recovery from brines. *Energy Environ. Sci.* **2012**, *5*, 9487−9491.
(37) Trócoli, R.; Battistel, A.; La Mantia, F. Nickel Hexacyanoferrate as Suitable Alternative to Ag for Electrochemical Lithium Recovery. *ChemSusChem* **2015**, *8*, 2514−2519.
(38) Hu, M.; Ishihara, S.; Ariga, K.; Imura, M.; Yamauchi, Y. Kinetically Controlled Crystallization for Synthesis of Monodispersed Coordination Polymer Nanocubes and Their Self-Assembly to Periodic Arrangements. *Chem. − Eur. J.* **2013**, *19*, 1882−1885.
(39) Chiang, Y. D.; Hu, M.; Kamachi, Y.; Ishihara, S.; Takai, K.; Tsujimoto, Y.; Ariga, K.; Wu, K. C. W.; Yamauchi, Y. Rational Design and Synthesis of Cyano-Bridged Coordination Polymers with Precise Control of Particle Size from 20 to 500 nm. *Eur. J. Inorg. Chem.* **2013**, *2013*, 3141−3145.
(40) Wu, X.; Sun, M.; Guo, S.; Qian, J.; Liu, Y.; Cao, Y.; Ai, X.; Yang, H. Vacancy-Free Prussian Blue Nanocrystals with High Capacity and Superior Cyclability for Aqueous Sodium-Ion Batteries. *ChemNanoMat* **2015**, *1*, 188−193.
(41) Wang, L.; Lu, Y.; Liu, J.; Xu, M.; Cheng, J.; Zhang, D.; Goodenough, J. B. A Superior Low-Cost Cathode for a Na-Ion Battery. *Angew. Chem., Int. Ed.* **2013**, *52*, 1964−1967.
(42) Wu, X.; Wu, C.; Wei, C.; Hu, L.; Qian, J.; Cao, Y.; Ai, X.; Wang, J.; Yang, H. Highly Crystallized $Na_2CoFe(CN)_6$ with Suppressed Lattice Defects as Superior Cathode Material for Sodium-Ion Batteries. *ACS Appl. Mater. Interfaces* **2016**, *8*, 5393−5399.

DOI: 10.1021/acsomega.6b00526
ACS Omega 2017, 2, 1653−1659